MARSIS Radar: Mars magnetic fields effects

Issue 1, Rev 0

PREPARED by : Marco Cartacci[1], Andrea Cicchetti[1], Raffaella Noschese[1]

CHECKED by : Roberto Orosei[2]

APPROVED by : Roberto Orosei[2]

[1]INAF-IAPS Via Fosso del Cavaliere 100, 00133, Rome, Italy
[2]INAF-IRA Via Piero Gobetti, 101, 40129 Bologna, Italy

1. Introduction

Mars is characterized by the absence of an intrinsic magnetic field like the Earth, but the presence of local crustal magnetic fields can produce an interaction with the ionosphere producing negative effects on the radar signal propagation. Taking into account the Ionosphere Density profiles available in Mars's literature [1]. and the observations of Mars from the Mars Global Surveyor (henceforth MGS), the purpose of this report is the evaluation of the magnetic fields impact on MARSIS and SHARAD signals.
The result of this report should be used in Operations Planning in order to select the optimum operative mode.

2. Mars magnetic fields

Mars have no appreciable global intrinsic magnetic fields, but the MGS has established that the planet has strong (up to 1600 nT) local magnetic fields(see fig. 1, 2 ,3, 4), probably related to properties in the martian crust [2].
The magnetic field lines of this crustal fields are closed in the lower ionosphere and the associated magnetic perturbations are detected also in the upper ionosphere.
Flux densities with strength exceeding 200 nT were measured at heights of 400 Km above the surface, but in some regions this influence arrive up to 700 Km.
In the above described scenario, the long wavelength and linearly polarized radar, MARSIS , could fly above a zone where the effects of both the magnetic field and the electron density in the ionosphere, in the worst case could combine.
In fact when the magnetic field is absent, wave propagation through the ionosphere is affected by the electron density of the plasma and the collision frequency between the electrons and ions. The interaction of this two factors altered the refractive index of the medium in an isotropic fashion and as a result the radio waves are slowed and attenuated. The introduction of the magnetic field in this system yields an alteration of the refractive index no more in an isotropic fashion and the result depend on the local magnetic field vector.
In general, when a linearly polarised wave propagates through the ionosphere, apart from possible attenuation of the wave, two major effects take place:

- The signal propagation is *perpendicular* (i.e. transverse) to the magnetic field. In this case the linear polarization becomes elliptical polarization and it is possible for the wave to become 100% circularly polarized.
- The signal propagation is *along* (i.e. longitudinal propagation) to the magnetic field. The plane of rotation is rotated. This is the *Faraday rotation*. Some ellipticity *can* also be introduced into a linearly polarized wave propagating along the magnetic field lines, under conditions of high ionospheric absorption..

The two cases are considered separately.

3. Propagation perpendicular to the magnetic field lines.

When the propagation occurs at right angles to the magnetic field, the E-field vector of the incident plane polarized wave can be considered as the superposition of two linearly polarized waves (see fig. 5), one with the E-field parallel to the magnetic field and the other with the E-field at right angles to the magnetic field. These waves are essentially the *ordinary* (*ord_w*), and the *extraordinary* (*ex_w*), components for propagation transverse to the magnetic field.

For the ordinary wave, the E-field accelerates electrons parallel to the magnetic field, which means that the magnetic field has no influence - a magnetic field only imposes a force on charged particles moving perpendicular to the field.

For the extraordinary wave, the E-field of the incident radiation accelerates the free electrons normal to the magnetic field, which then exerts a force on the electrons and so modifies the electronic motion. This causes the ionospheric refractive index for the extraordinary wave to be different from that of the ordinary wave, and also to vary according to the magnetic field.

The different refractive indices of the two component waves, meaning different propagation velocities, causes a progressive phase shift between the two components. If this phase shift becomes 90 degrees, then the initial 100% linearly polarized wave have been turned into a 100% circularly polarized wave.

The ionosphere can also introduced a different attenuation for the two component waves and then the initial linearly polarized wave could become an elliptically polarized wave. (We have an elliptically polarized wave when the amplitudes of the two components differ and the phase shift is $\Phi = 0 \div 2\pi$.)

1.1 MARSIS implications.

The absorption of ionosphere to the sounding wave with magnetic fields is calculated following:

1) $$A = 4.6 \cdot 10^{-5} \int \frac{N(z) \cdot \upsilon(z)}{(\omega \pm \omega_c)^2 + \upsilon^2(z)} dz \qquad (dB)$$

where $N(z)$ is the electron density in m^{-3}, $\nu(z)$ is the electron-neutral collision frequency, ω is the angular frequency of the sounding wave, and ω_c is the angular gyrofrequency corresponding to the vertical component of the magnetic field, and $\pm$ means there are two branches of wave in the magnetic field, z is the altitude.

From [3] and [4] we know also that, since $\omega_c << \omega$, the ionospheric absorption due to the magnetic field is too low to have noticeable effect. Then there is not a differential absorption between the ordinary and the extraordinary waves and an eventual phase shift would not yield elliptical polarization.

In conclusion for MARSIS the elliptical polarization is not a problem.

1.2 SHARAD implications.

Since the operative frequency of SHARAD (f_0 = 15 ÷ 25 MHz) it is higher than MARSIS (f_0 = 5 MHz in Band IV), the elliptical polarization is not a problem for SHARAD too.

3 Propagation along to the magnetic field lines.

3.1FARADAY ROTATION

In Operations Planning the Martian magnetic field may require consideration in as far it causes faraday rotation of the radar signal. If the rotation is near 90 degrees fadings of the signal results. In this section an estimate for the expected Faraday rotation angle for linearly polarized radio waves propagating in the Martian ionosphere will be provided. These calculations take advantage of recent vector magnetic field measurements by Mars Global Surveyor (MGS) to provide an overall impact on Marsis and Sharad operations.

The Faraday rotation angle is directly dependent on the normal magnetic field and local electron density. The rotation angle in radians is given by (MKS units).
Below we expose two different approaches with the same final result.

For a linearly polarized wave propagating *along* the magnetic field lines in the ionosphere, it is convenient to consider the wave as the sum of two circularly polarized waves (see fig. 6), one LHCP (Left Hand Circularly Polarized) and the other RHCP (Right Hand Circularly Polarized). The combination equal amplitude LHCP and RHCP waves is a 100% linearly polarized wave. **The relative phase difference between the RHCP and LHCP components determines the position angle of the E-field of the linearly polarized wave after the summation.** A difference in refractive index, or velocity of propagation, for the RHCP and LHCP components will lead to a gradual rotation of the linearly polarized E-field vector. This is just normal *Faraday Rotation.*

For a circularly polarized wave, the refractive index of the medium with the presence of the magnetic field can be expressed as:

2) $$n_{\pm}^2 = 1 - \frac{f_p^2}{f\left(f \pm f_c\right) - if\nu} \cong 1 - \frac{f_p^2}{f\left(f \pm f_c\right)}$$

Assuming $f_p < f$ we have:

3) $$n_{\pm}(z)=\sqrt{1-\frac{f_p^2(z)}{f\left(f\pm f_c\right)}}\cong 1-\frac{1}{2}\left(\frac{f_p^2(z)}{f\left(f\pm f_c\right)}\right)-\frac{1}{8}\left(\frac{f_p^4(z)}{f^2\left(f\pm f_c\right)^2}\right)$$

The cyclotron frequency of an electron moving in a magnetic field is related to the strength of the magnetic field and is given by:

4) $$\omega_c=\frac{q_e}{m_e}B_n \qquad \rightarrow \qquad f_c=\frac{1}{2\pi}\cdot\frac{q_e}{m_e}B_n$$

$q_e = 1.6\ 10^{-19}$ C , electron charge

$m_e = 9.1\ 10^{-31}$ Kg , electron mass

B_n = magnetic field normal to the motion of the electron

Note that the Faraday rotation angle does not depend on the collision frequency since $v << f$.
The one-way polarization angle rotation rate can be written as:

5) $$\frac{d\Psi}{dz}=\frac{k}{2}\left(n_+(z)-n_-(z)\right) \qquad \rightarrow \quad k=\frac{2\pi}{\lambda}=\frac{2\pi f}{c}$$

where k is the wave number and c is the light speed in the vacuum.
The total polarization angle rotation can be calculated by integrating the above equation over the propagation length.

6) $$\Psi=\frac{k}{2}\int_0^h\left(n_+(z)-n_-(z)\right)dz$$

7) $$n_+(z)-n_-(z)=\frac{1}{2}\cdot\frac{f_p^2(z)}{f}\left(\frac{1}{f-f_c}-\frac{1}{f+f_c}\right)+\frac{1}{8}\cdot\frac{f_p^4(z)}{f^2}\left(\frac{1}{(f-f_c)^2}-\frac{1}{(f+f_c)^2}\right)\cong$$
$$\cong\frac{f_c}{f^3}\left(f_p^2(z)+\frac{1}{2}\cdot\frac{f_p^4(z)}{f^2}\right)$$

The Faraday rotation angle directly depends on the normal magnetic field and local electron density (or quadratic dependence on the plasma frequency f_p). Since the magnetic field is locally stable, the main source of variation in the Faraday rotation angle is the solar zenith angle at the time of observation.
From 6) we have:

8) $$\Psi = \frac{k}{2}\frac{f_c}{f^3}\left(\int_0^h f_p^2(z)\,dz + \frac{1}{2f^2}\int_0^h f_p^4(z)\,dz\right) = \frac{q_e}{2cm_e}\cdot(8.98)^2\cdot\frac{B_n}{f^2}\left(\int_0^h n_e(z)\,dz + \frac{(8.98)^2}{2f^2}\int_0^h n_e^2(z)\,dz\right)$$

9) $$\Psi \cong 2.36\cdot10^4\cdot\frac{B_n}{f^2}\int_0^h n_e(z)\,dz = 2.36\cdot10^4\cdot\frac{B_n}{f^2}\cdot TEC$$

where integral is along the ray path, and 'B_n' is the normal magnetic field magnitude.

The Faraday rotation angle is given by :

10) $$\Psi = 2.36\cdot10^4\,\frac{1}{f^2}\int_0^h B\cos\theta\cdot\sec\varphi\cdot n_e(z)dz$$

where integral is along the ray path.

B = normal magnetic field magnitude

θ = angle between B and signal k-vector

φ = angle between k-vector and vertical

For Marsis and Sharad we have φ=0.
Assume that B cos θ can be replaced by a mean value < B cos θ> ; this will possibly produce an upper estimate of the rotation. Now we have for θ = 90º

11) $$\Psi \approx 2.36\cdot10^4\,\frac{<B\cos\theta>}{f^2}\int_0^h n_e(z)dz = 2.36\cdot10^4\,\frac{<B\cos\theta>}{f^2}TEC = 2.36\cdot10^4\,\frac{B_n}{f^2}TEC$$

Assuming for TEC the following expression:

12) $$TEC = \int_0^h n_e(z)dz$$

with:

13) $$n_e(z) = n_{e,\max}\left(\frac{z-h_0}{b}\right)^2\cdot\exp\left[2\cdot\left(1-\frac{z-h_0}{b}\right)\right], \quad z \ge h_0$$ *Electron Density*

where:

14) $$n_{e,\max} = \left(\frac{f_{p,\max}}{8.98} \right)^2$$

$f_{p,max}$ = maximum plasma frequency;

b = shape factor;

$h_0 = 0$, beginning of the ionosphere layer, this value is necessary because the TEC integration interval start from 0 up to h (height of S/C);

3.2 MARSIS implications.

Then we have for example:

$TEC \cong 4.39 \cdot 10^{14}$ *for* $f_0 = 1.8\,MHz$, $f_{p,\max} = 1MHz$, $b = 20\,Km$;

$TEC \cong 1.1 \cdot 10^{15}$ *for* $f_0 = 1.8\,MHz$, $f_{p,\max} = 1MHz$, $b = 50\,Km$;

$TEC \cong 1.1 \cdot 10^{16}$ *for* $f_0 = 1.8\,MHz$, $f_{p,\max} = 5\,MHz$, $b = 20\,Km$;

$TEC \cong 2.74 \cdot 10^{16}$ *for* $f_0 = 1.8\,MHz$, $f_{p,\max} = 5\,MHz$, $b = 50\,Km$;

Now as we can see in fig. 1 the Mars normal magnetic field strength is less of 50 nT for the major part of the planet. A more accurate estimation [2] show that the magnetic field is noticeably lower in the northern hemisphere where 80% of the measurements were below 20 nT in comparison to 60 nT for the southern hemisphere.

It must be pointed out that the values given in MAG/ER are valid at 400 km from the Mars surface. It has to be expected that the maximum value of magnetic field will be within 300 km and 50 km where it can overcome the values on figure 1 (where $B_r \equiv B_n$). Then in the present calculation the magnetic field strength has been assumed as a value from 50 nT up to 1000 nT.
Remembering that the attenuation due to the signal polarization rotation is:

15) $$A = 20 \log_{10}(\cos(\Psi))$$

we can see in fig. 7, 8, 9, 10, 11 the behaviors of the Faraday rotation angle and the relative attenuation for some representative values of the magnetic field strength (B= 50, 200, 500, 1000 nT) and also the negative influence of higher plasma frequencies.

In conclusion the use of the lowest band would seem possible only for higher solar zenith angles (night time) and areas with weak magnetic fields, but also with higher bands could be some problems, if there were combinations of high plasma frequency and/or strong magnetic fields .

3.3 SHARAD implications.

Using the same formulas 9), 11) and 15) we can estimate the impact of the Farady Rotation on SHARAD.
How shown in figg.12a,b,c,d for night-side operations with the maximum value of plasma frequency ($f_{p,max}$ = 1 MHz), there is no problem at all, also for normal magnetic field values very high.
Moreover figg. 13, 14 show that in day-side operations, the combination of the maximum plasma frequency ($f_{p,max}$ = 4 - 5 MHz) and a magnetic field strength $B_n \geq 500$ nT will lead to heavy attenuations.
In conclusion, even if for day-side operations, the magnetic fields represents a serious constraint also for SHARAD.

Note: If one of the circularly polarized component terms is attenuated more than the other, then the sum of the RHCP and LHCP terms will no longer give pure 100% linear polarization. In other words, differential absorption between the LHCP and RHCP waves could introduce ellipticity into the polarization of the wave, but from [3] and [4] we know also that, since $\omega_c << \omega$, the ionospheric absorption difference between the two wave branches is too low to have noticeable effect.

References

[1] Gurnett D. A., Huff R. L., Morgan D. D., Persoon A. M., Averkamp T. F., Kirchner D. L., Duru F., Akalin F., Kopf A. J., Nielsen E., Safaeinili A., Plaut J. J. and Picardi G., 2007: An overview of radar soundings of the martian ionosphere from the Mars Express spacecraft, Advances in Space Research 41, 1335-1346.

[2] Lillis R. J., Frey H. V., Manga M., Mitchell D. L., Lin R. P., Acuna M. H., Bougher S. W.: An improved crustal magnetic field map of Mars from electron reflectometry: Highland volcano magmatic history and the end of the martian dynamo, Icarus 194 (2008) 575-596.

[3] Safaeinili, A., Kofman, W., Nouvel, J. F., Herique, A., Jordan, R. L., 2003: Impact of Mars ionosphere on orbital radar sounder operation and data processing, Planetary and Space Science, Volume 51, Issue 7-8, p. 505-515, 2003.

[4] Safaeinili, A., Kofman, W., Mouginot, J., Gim, Y., Herique, A., Ivanov, A. B., Plaut, J. J., and Picardi, G. , 2007: Estimation of the total electron content of the Martian ionosphere using radar sounder surface echoes, Geophysical Research Letters, Vol. 34

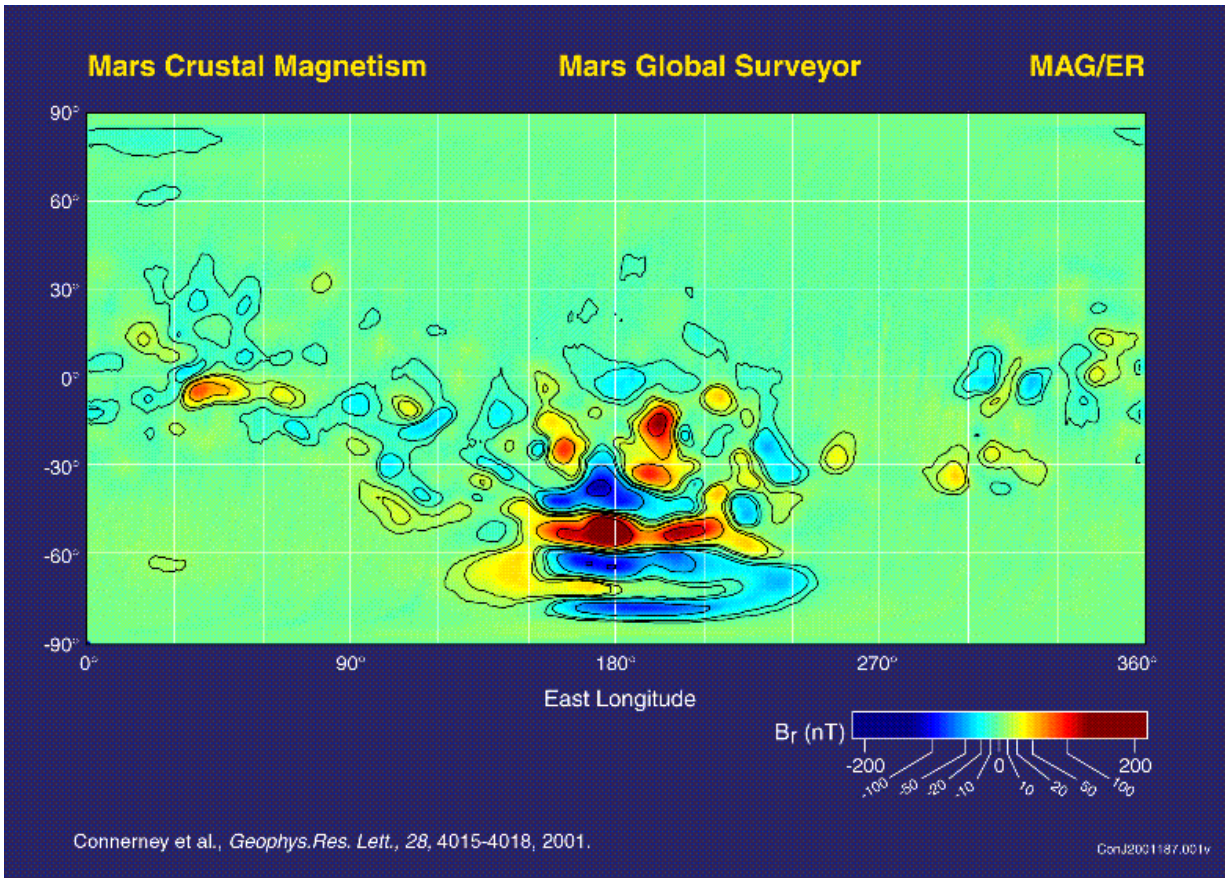
Mars Crustal Magnetism
Mars Global Surveyor
MAG/ER
90°
60°
30°
0°
-30°
-60°
-90°
0°
90°
180°
270°
360°
East Longitude
Br (nT)
-200
-100
-50
-20
-10
0
10
20
50
100
200
Connerney et al., Geophys.Res. Lett., 28, 4015-4018, 2001.

Fig. 1

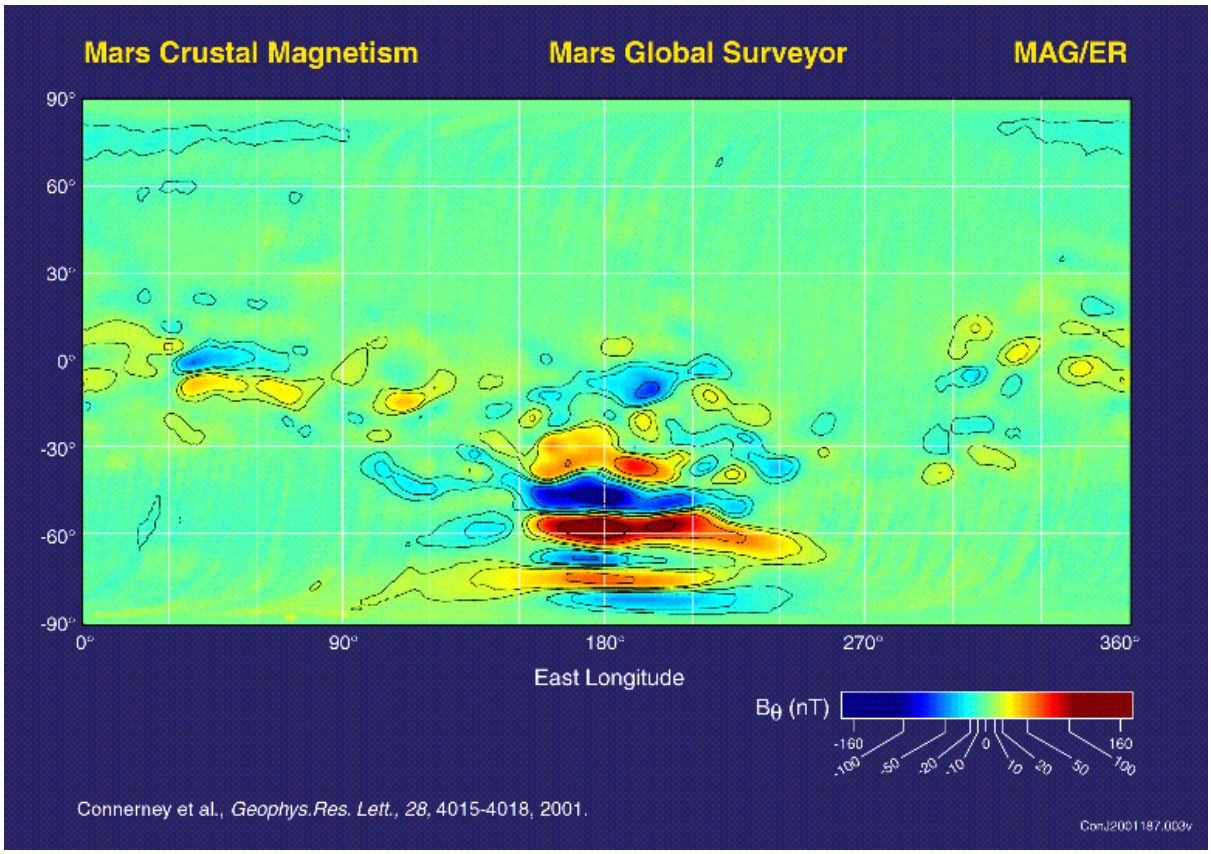
Mars Crustal Magnetism
Mars Global Surveyor
MAG/ER
90°
60°
30°
0°
-30°
-60°
-90°
0°
90°
180°
270°
360°
East Longitude
Bθ (nT)
-160
-100
-50
-20
-10
0
10
20
50
100
160
Connerney et al., Geophys.Res. Lett., 28, 4015-4018, 2001.

Fig. 2

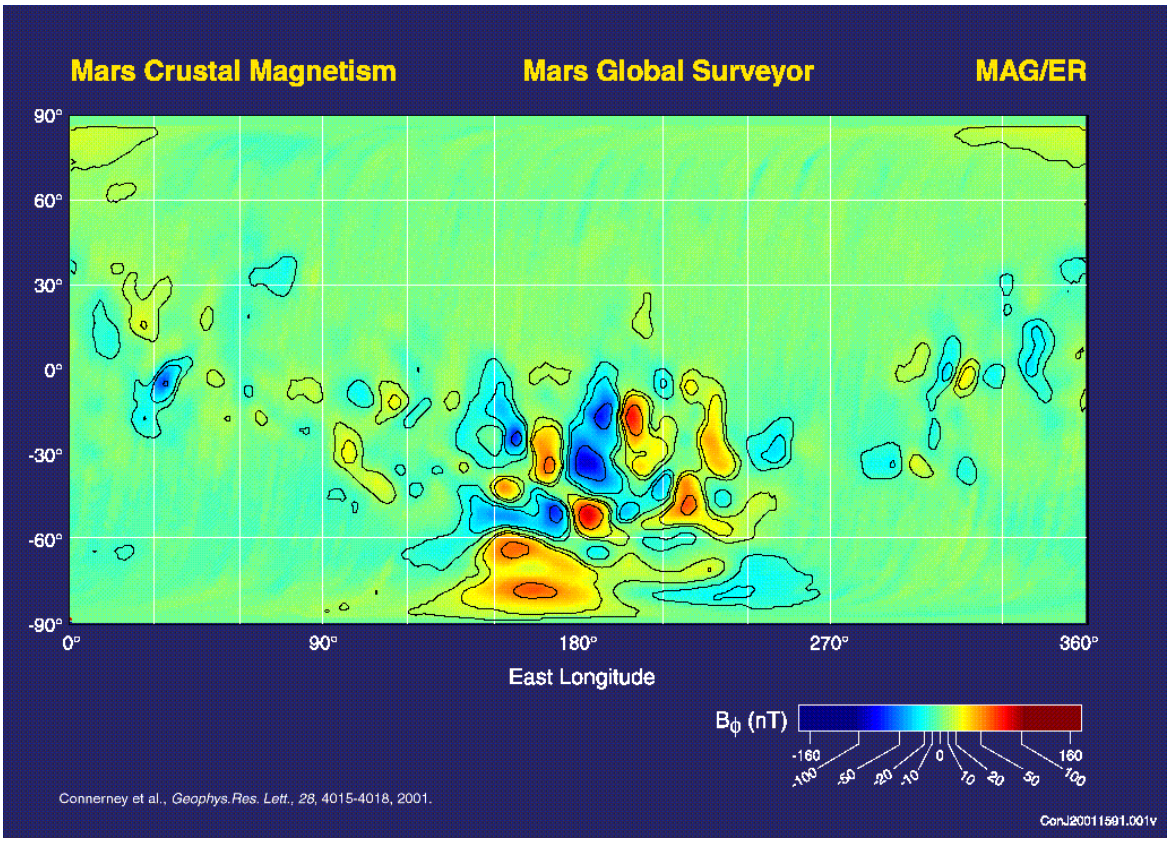
Mars Crustal Magnetism
Mars Global Surveyor
MAG/ER
90°
60°
30°
0°
-30°
-60°
-90°
0°
90°
180°
270°
360°
East Longitude
Bϕ (nT)
-160
-100
-50
-20
-10
0
10
20
50
100
160
Connerney et al., Geophys.Res. Lett., 28, 4015-4018, 2001.
ConJ20011501.001v

Fig. 3

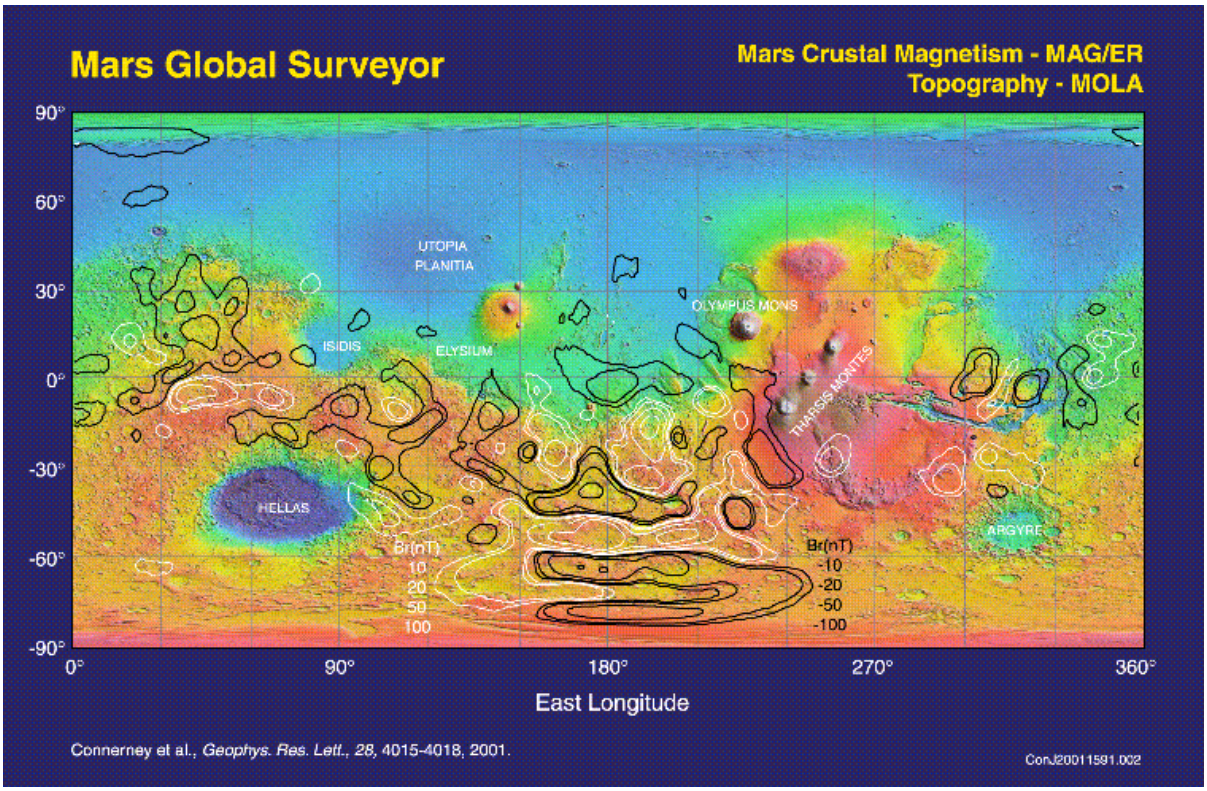
Mars Global Surveyor
Mars Crustal Magnetism - MAG/ER
Topography - MOLA
90°
60°
30°
0°
-30°
-60°
-90°
UTOPIA
PLANITIA
ISIDIS
ELYSIUM
OLYMPUS MONS
THARSIS MONTES
HELLAS
ARGYRE
Br(nT)
10
20
50
100
Br(nT)
-10
-20
-50
-100
0°
90°
180°
270°
360°
East Longitude
Connerney et al., Geophys. Res. Lett., 28, 4015-4018, 2001.
ConJ20011591.002

Fig. 4

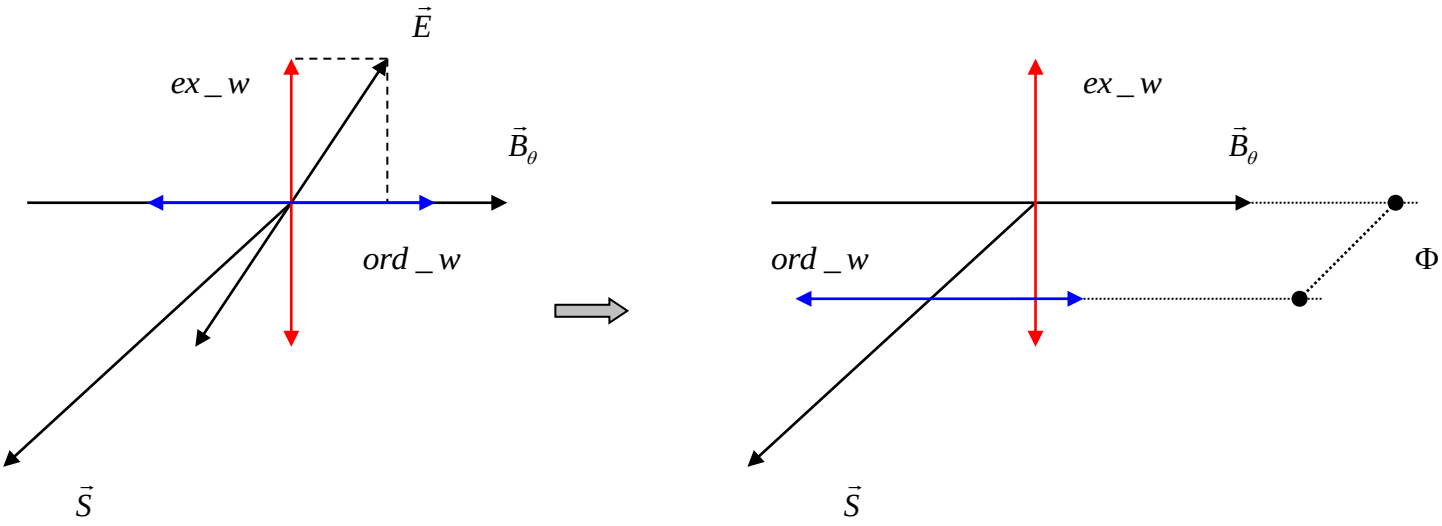
$\vec{E}$
ex _ w
$\vec{B}_\theta$
ord _ w
$\vec{S}$
ex _ w
$\vec{B}_\theta$
ord _ w
Φ
$\vec{S}$

Fig. 5

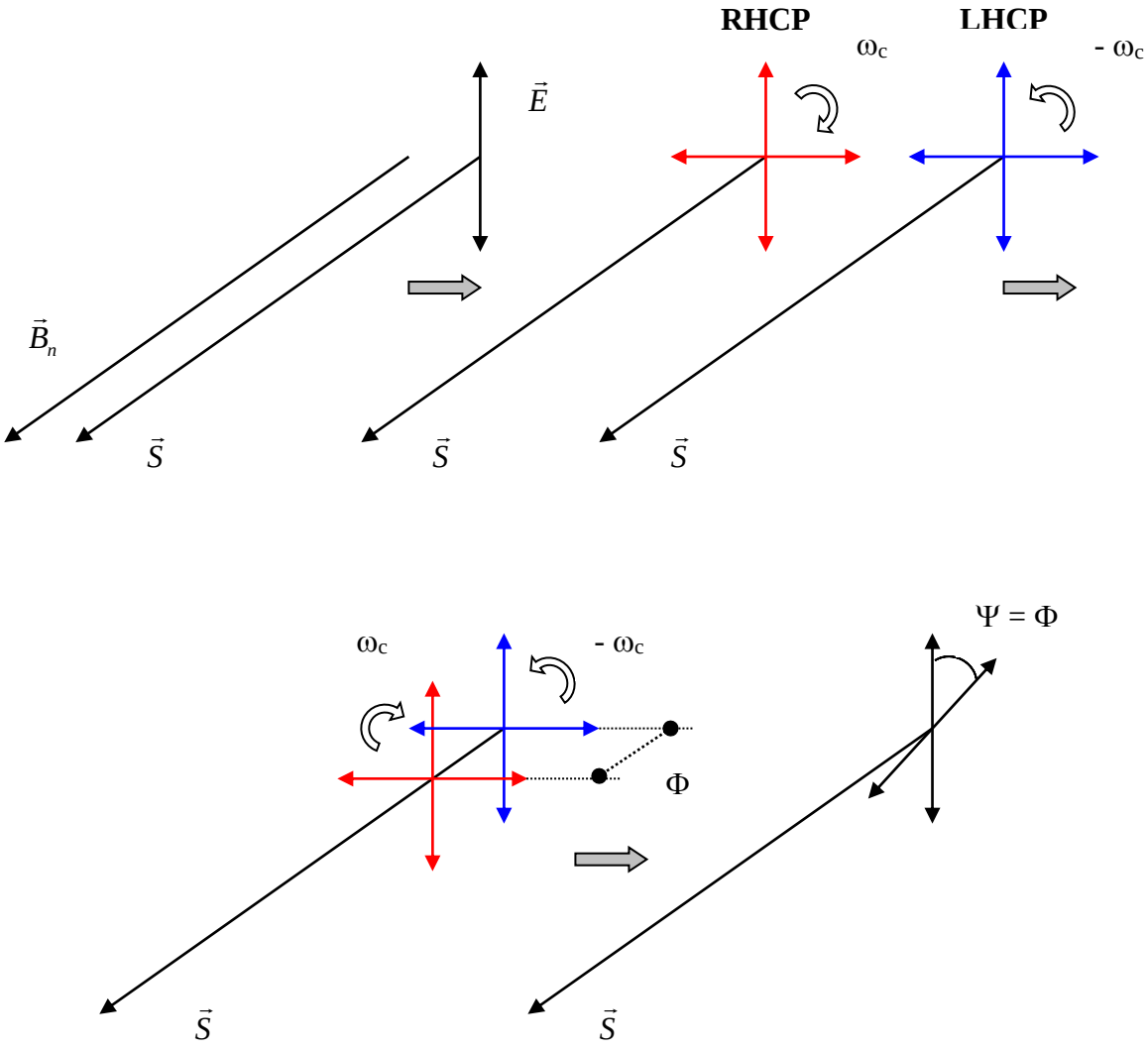
RHCP
LHCP
ωc
- ωc
$\vec{E}$
$\vec{B}_n$
$\vec{S}$
$\vec{S}$
$\vec{S}$
ωc
- ωc
Φ
Ψ = Φ
$\vec{S}$
$\vec{S}$

Fig. 6

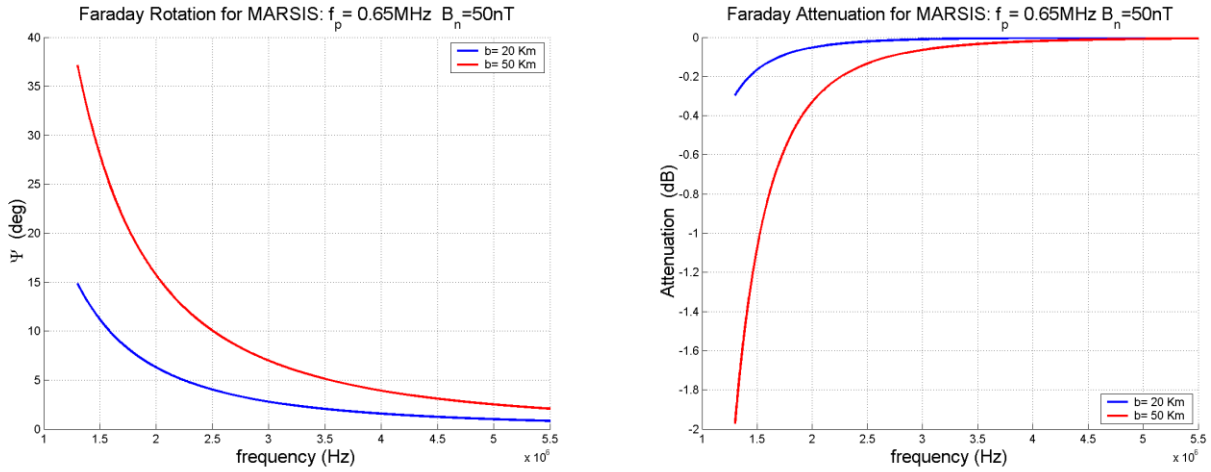
Faraday Rotation for MARSIS: f_p = 0.65MHz B_n=50nT
Ψ (deg)
frequency (Hz)
x 10^6
b= 20 Km
b= 50 Km
Faraday Attenuation for MARSIS: f_p = 0.65MHz B_n=50nT
Attenuation (dB)
frequency (Hz)
x 10^6
b= 20 Km
b= 50 Km

Fig. 7a

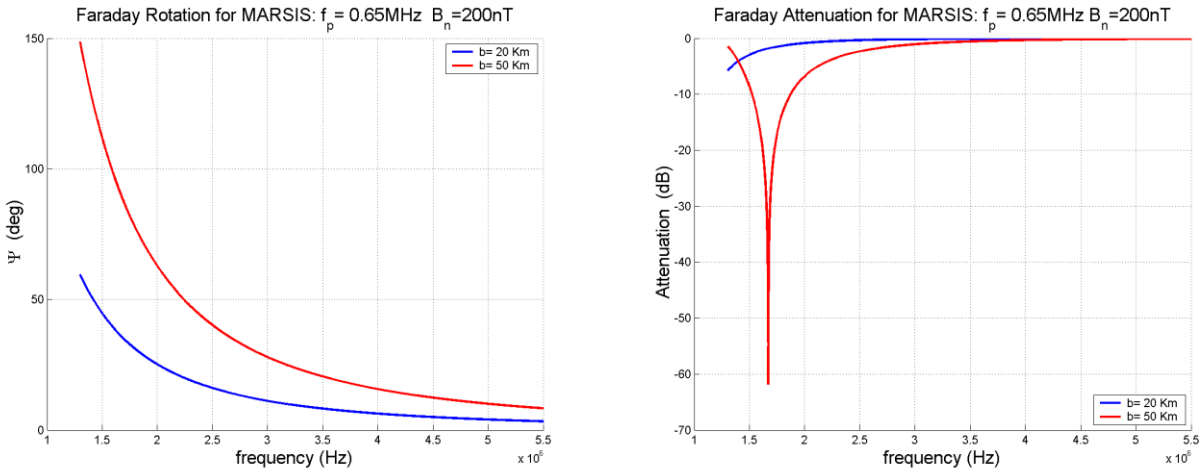
Faraday Rotation for MARSIS: f_p = 0.65MHz B_n=200nT
Ψ (deg)
frequency (Hz)
x 10^6
b= 20 Km
b= 50 Km
Faraday Attenuation for MARSIS: f_p = 0.65MHz B_n=200nT
Attenuation (dB)
frequency (Hz)
x 10^6
b= 20 Km
b= 50 Km

Fig. 7b

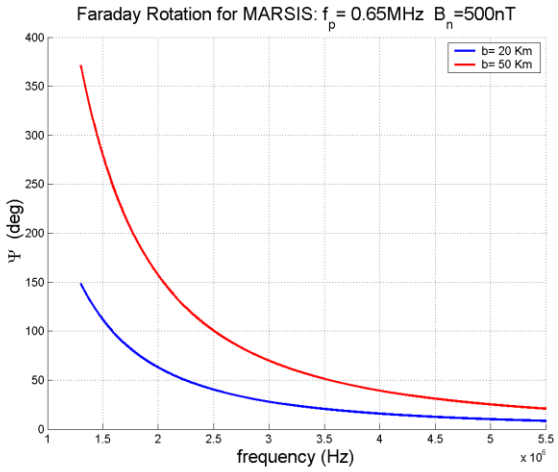
Faraday Rotation for MARSIS: f_p = 0.65MHz B_n=500nT
b= 20 Km
b= 50 Km
Ψ (deg)
frequency (Hz)
x 10^6

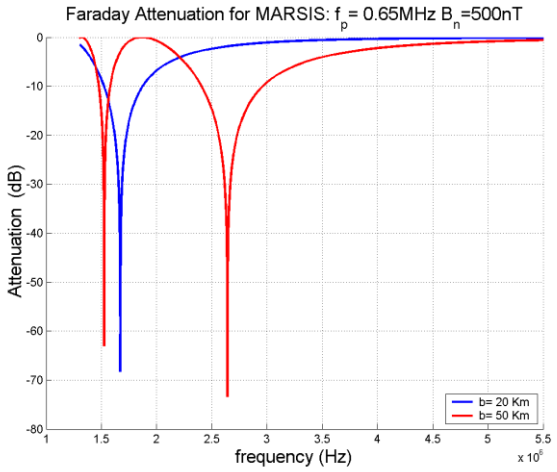
Faraday Attenuation for MARSIS: f_p = 0.65MHz B_n=500nT
Attenuation (dB)
b= 20 Km
b= 50 Km
frequency (Hz)
x 10^6

Fig. 7c

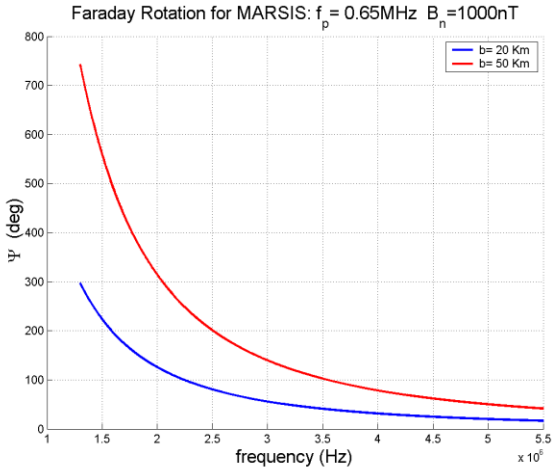
Faraday Rotation for MARSIS: f_p = 0.65MHz B_n=1000nT
b= 20 Km
b= 50 Km
Ψ (deg)
frequency (Hz)
x 10^6

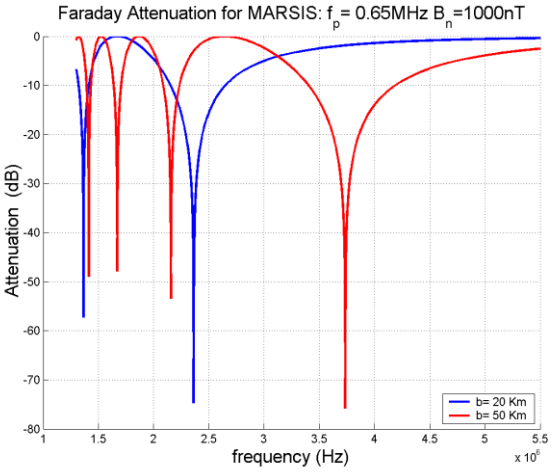
Faraday Attenuation for MARSIS: f_p = 0.65MHz B_n=1000nT
Attenuation (dB)
b= 20 Km
b= 50 Km
frequency (Hz)
x 10^6

Fig. 7d

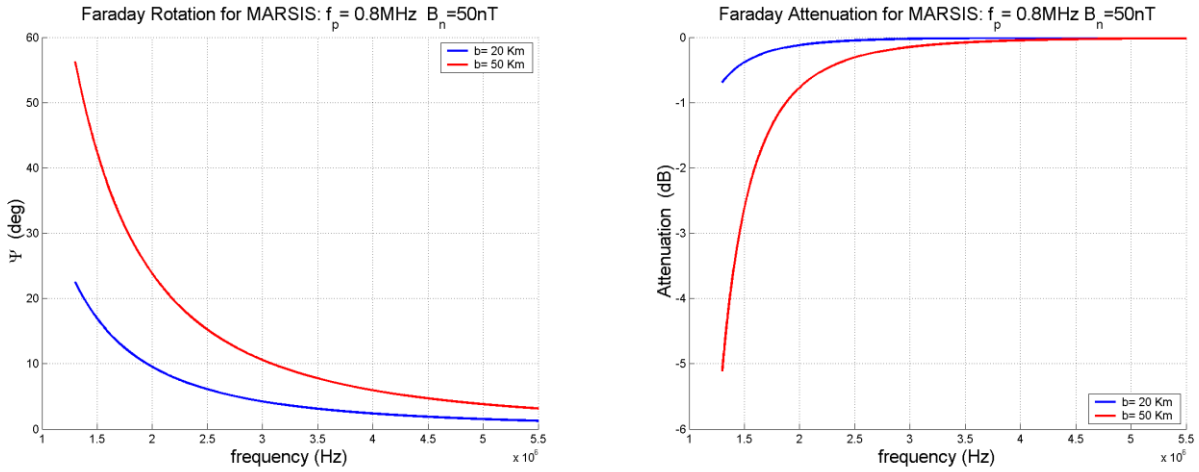
Faraday Rotation for MARSIS: f_p = 0.8MHz B_n=50nT
b= 20 Km
b= 50 Km
Ψ (deg)
frequency (Hz)
x 10^6
Faraday Attenuation for MARSIS: f_p = 0.8MHz B_n=50nT
Attenuation (dB)
b= 20 Km
b= 50 Km
frequency (Hz)
x 10^6

Fig. 8a

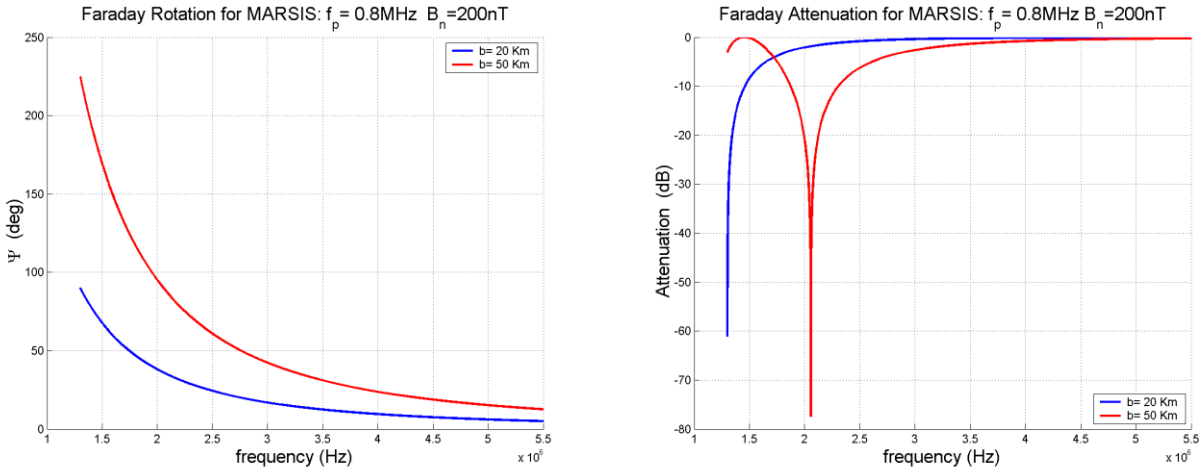
Faraday Rotation for MARSIS: f_p = 0.8MHz B_n=200nT
b= 20 Km
b= 50 Km
Ψ (deg)
frequency (Hz)
x 10^6
Faraday Attenuation for MARSIS: f_p = 0.8MHz B_n=200nT
Attenuation (dB)
b= 20 Km
b= 50 Km
frequency (Hz)
x 10^6

Fig. 8b

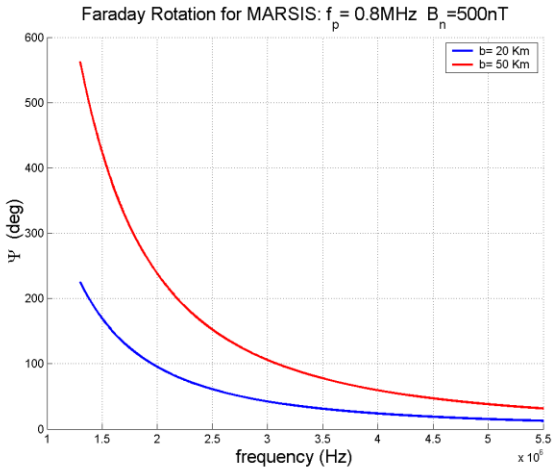
Faraday Rotation for MARSIS: f_p = 0.8MHz B_n=500nT
b= 20 Km
b= 50 Km
Ψ (deg)
frequency (Hz)
x 10^6

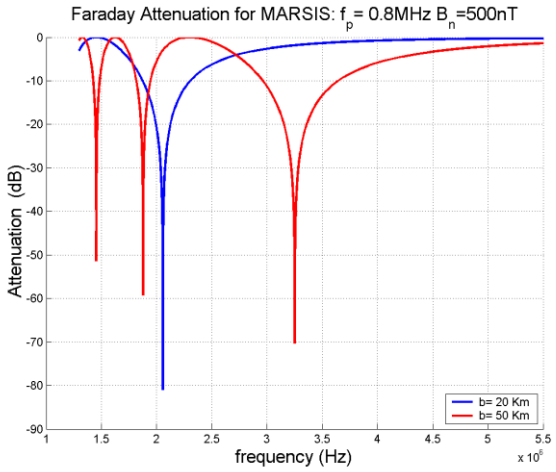
Faraday Attenuation for MARSIS: f_p = 0.8MHz B_n=500nT
b= 20 Km
b= 50 Km
Attenuation (dB)
frequency (Hz)
x 10^6

Fig. 8c

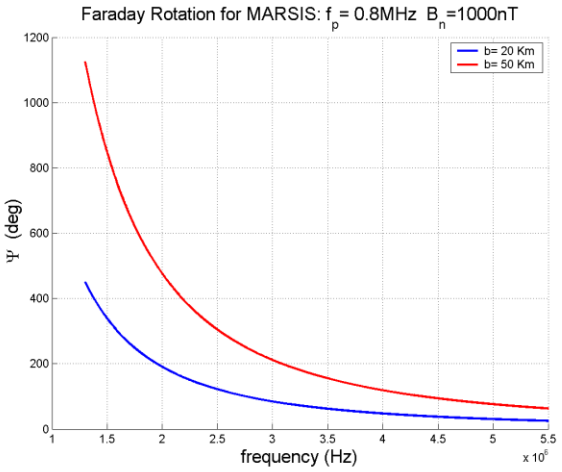
Faraday Rotation for MARSIS: f_p = 0.8MHz B_n=1000nT
b= 20 Km
b= 50 Km
Ψ (deg)
frequency (Hz)
x 10^6

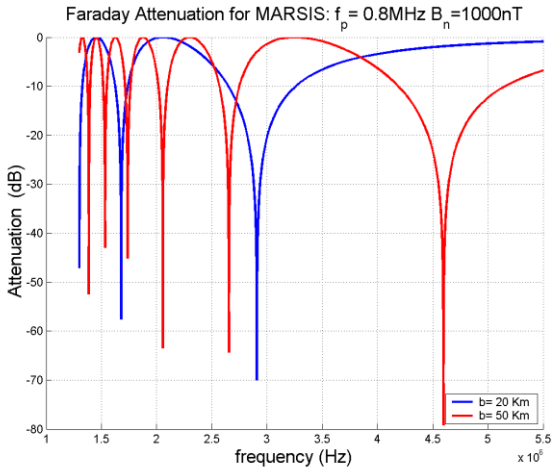
Faraday Attenuation for MARSIS: f_p = 0.8MHz B_n=1000nT
b= 20 Km
b= 50 Km
Attenuation (dB)
frequency (Hz)
x 10^6

Fig. 8d

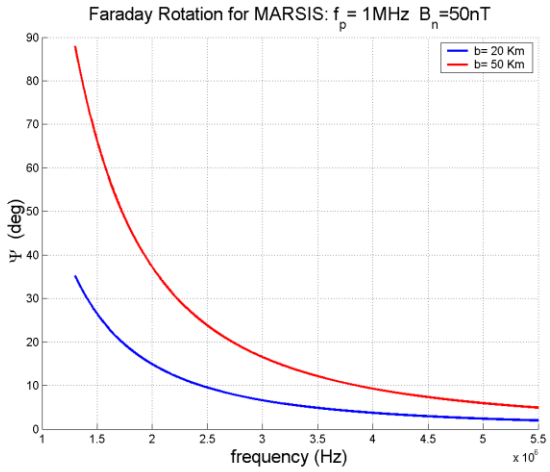
Faraday Rotation for MARSIS: f_p= 1MHz B_n=50nT
b= 20 Km
b= 50 Km
Ψ (deg)
frequency (Hz)
x 10^6

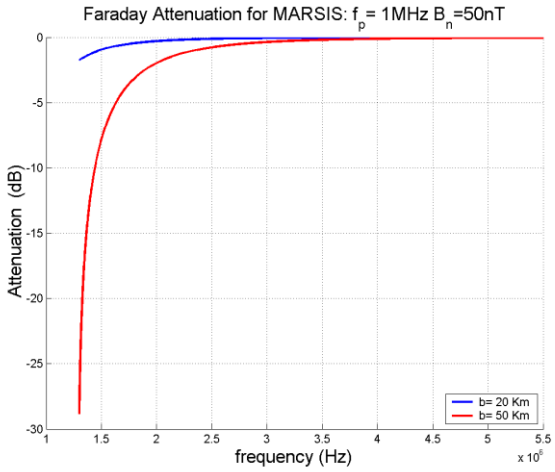
Faraday Attenuation for MARSIS: f_p= 1MHz B_n=50nT
b= 20 Km
b= 50 Km
Attenuation (dB)
frequency (Hz)
x 10^6

Fig. 9a

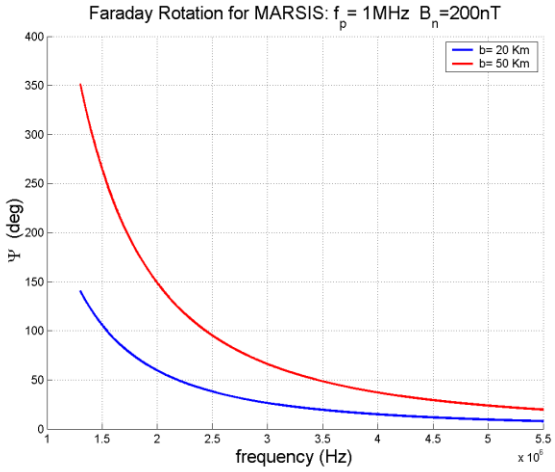
Faraday Rotation for MARSIS: f_p= 1MHz B_n=200nT
b= 20 Km
b= 50 Km
Ψ (deg)
frequency (Hz)
x 10^6

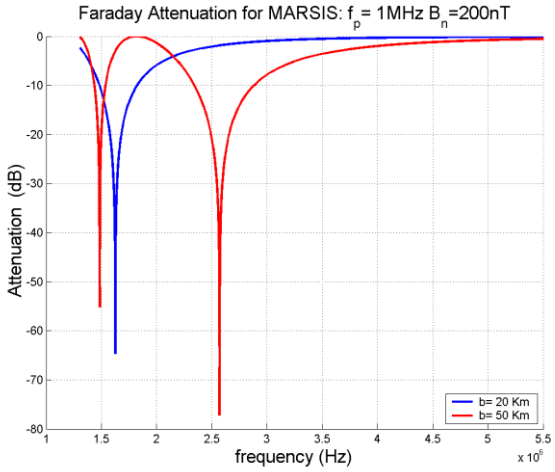
Faraday Attenuation for MARSIS: f_p= 1MHz B_n=200nT
b= 20 Km
b= 50 Km
Attenuation (dB)
frequency (Hz)
x 10^6

Fig. 9b

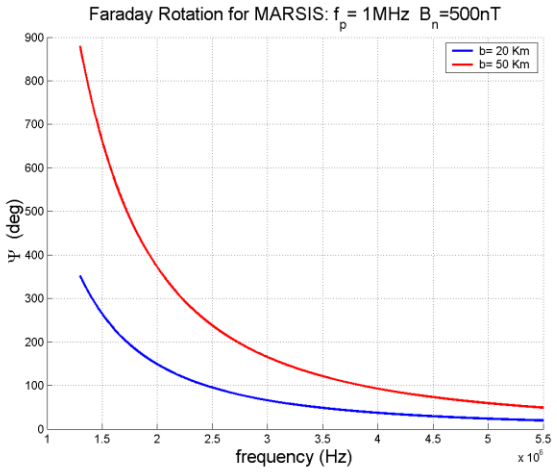
Faraday Rotation for MARSIS: f_p = 1MHz B_n=500nT
b= 20 Km
b= 50 Km
Ψ (deg)
frequency (Hz)
x 10^6

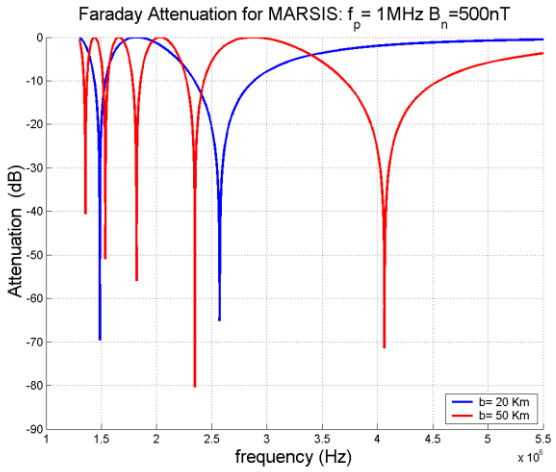
Faraday Attenuation for MARSIS: f_p = 1MHz B_n=500nT
Attenuation (dB)
b= 20 Km
b= 50 Km
frequency (Hz)
x 10^6

Fig. 9c

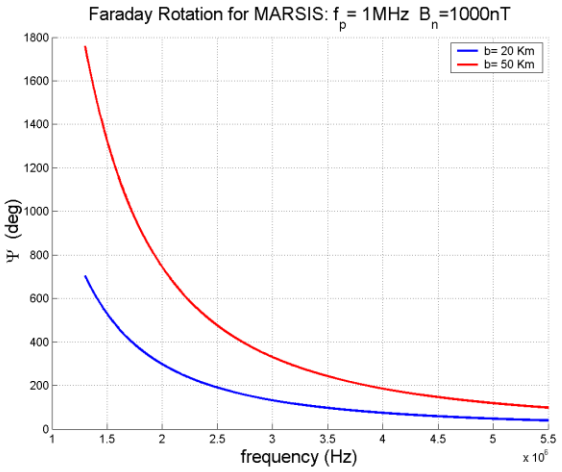
Faraday Rotation for MARSIS: f_p = 1MHz B_n=1000nT
b= 20 Km
b= 50 Km
Ψ (deg)
frequency (Hz)
x 10^6

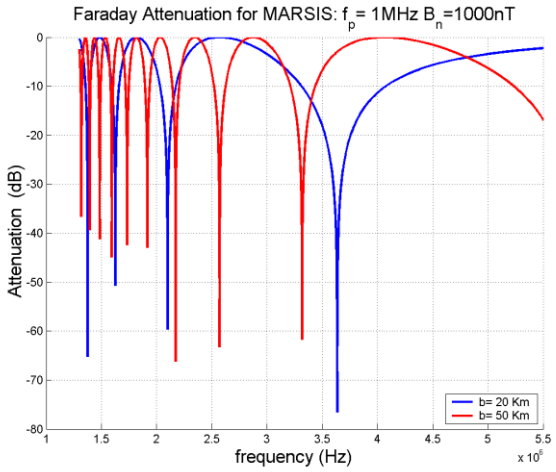
Faraday Attenuation for MARSIS: f_p = 1MHz B_n=1000nT
Attenuation (dB)
b= 20 Km
b= 50 Km
frequency (Hz)
x 10^6

Fig. 9d

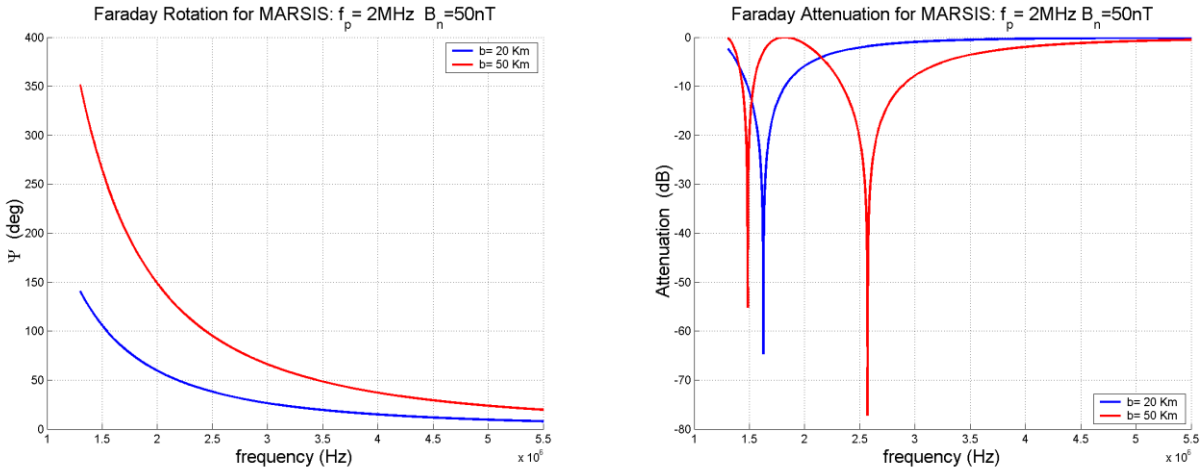

Fig. 10a

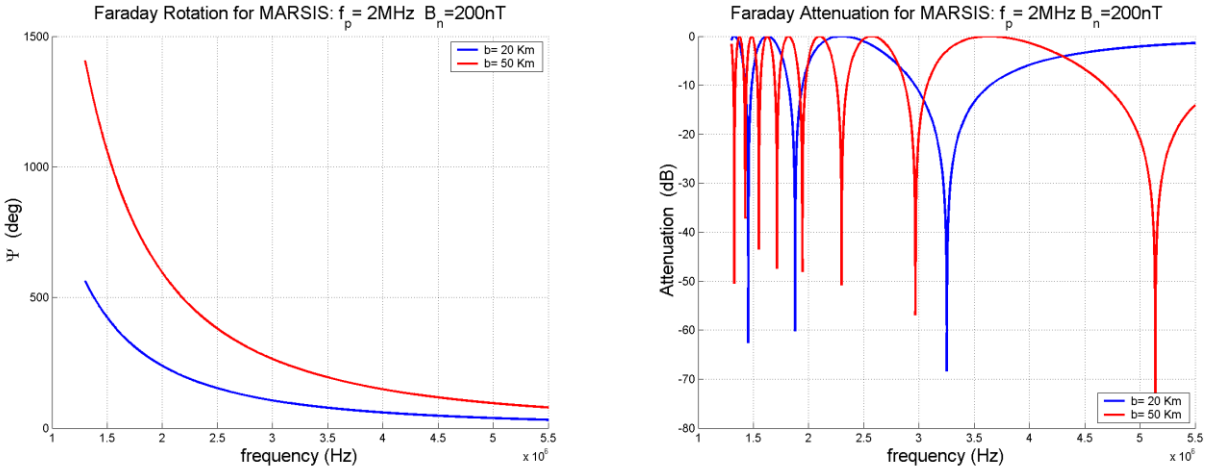

Fig. 10b

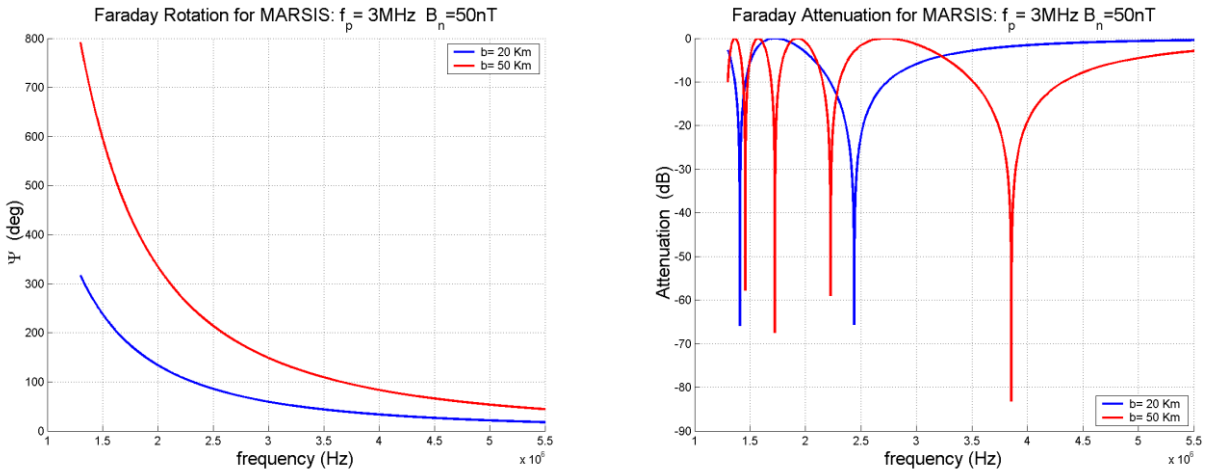

Fig. 11

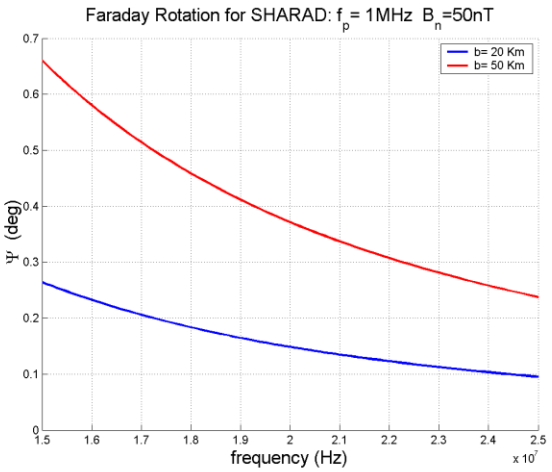

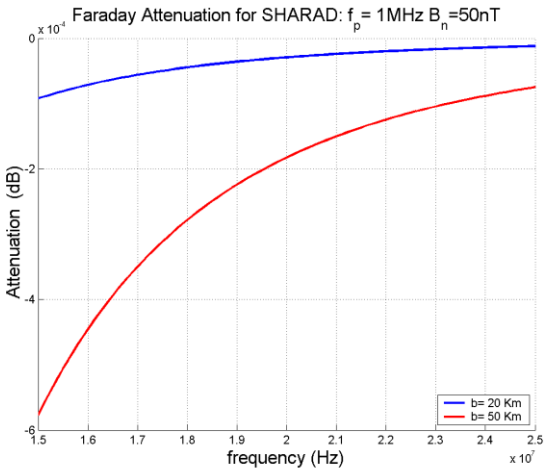

Fig. 12a

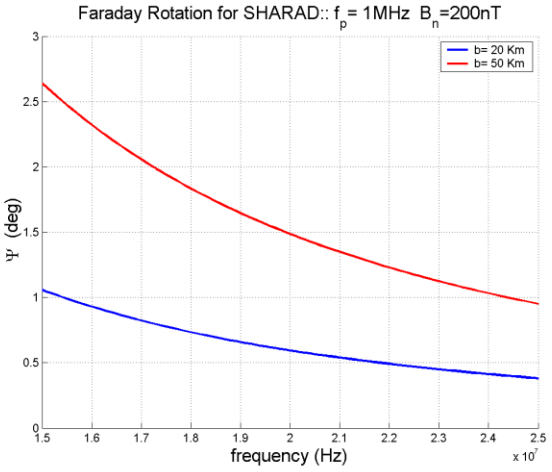

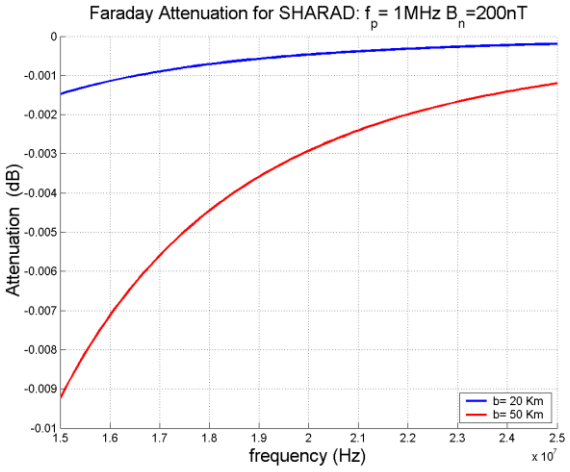

Fig. 12b

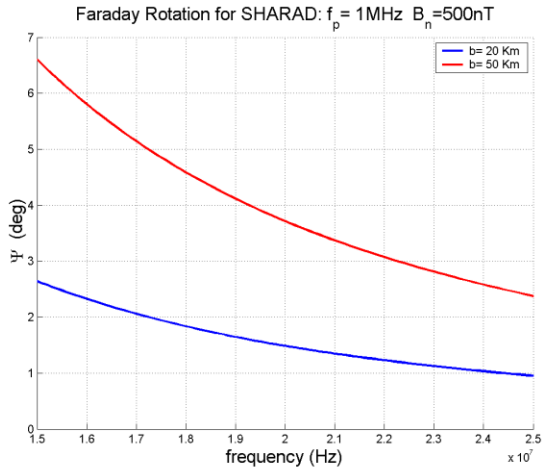

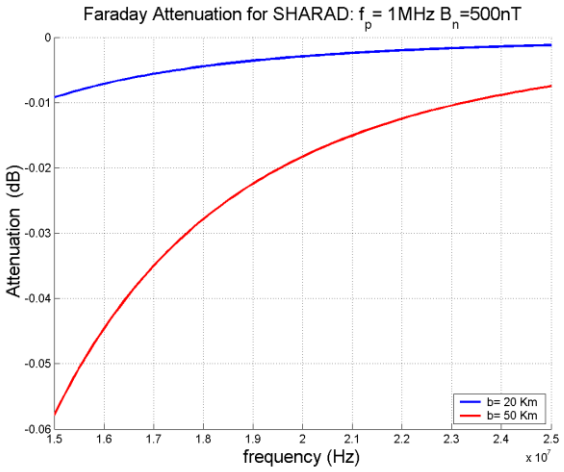

Fig. 12c

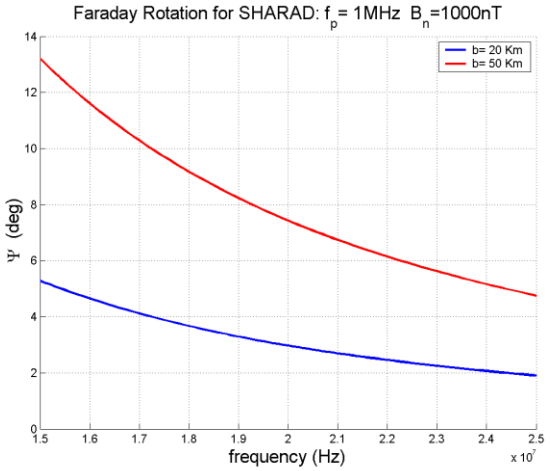

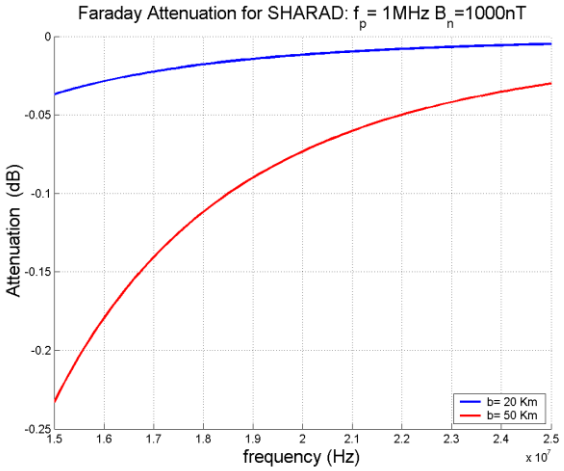

Fig. 12d

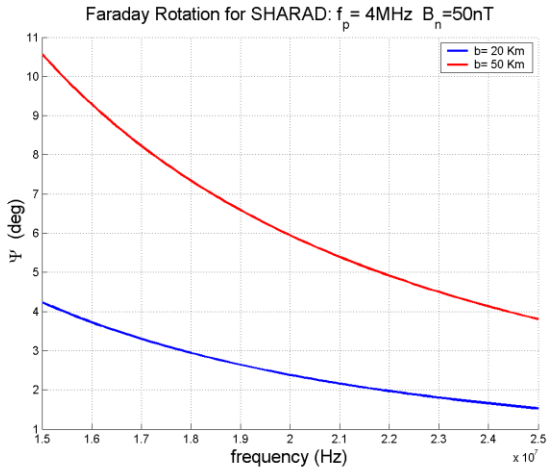

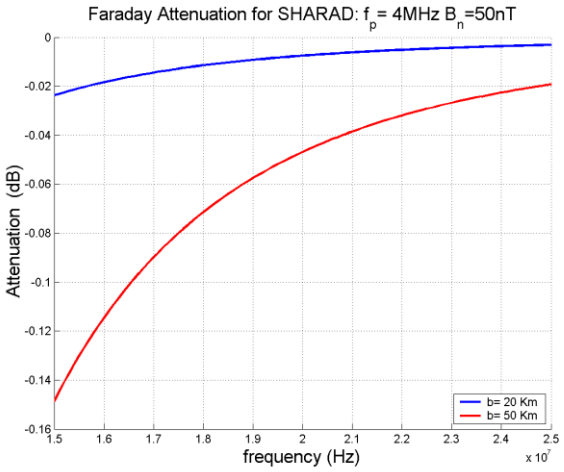

Fig. 13a

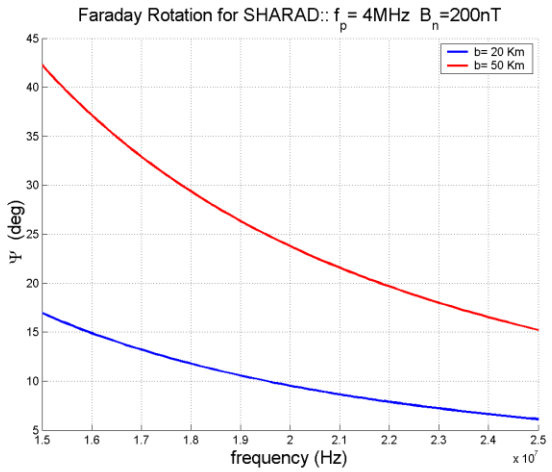

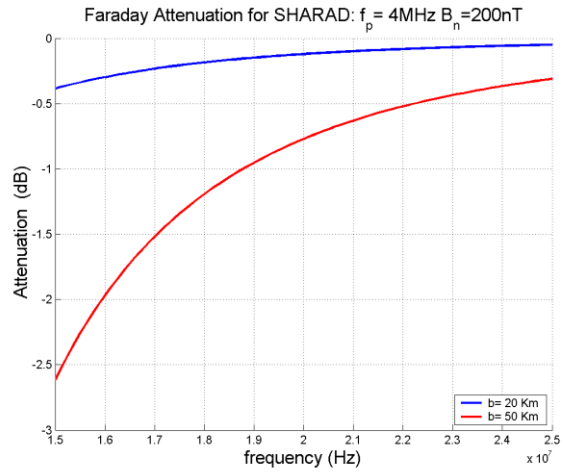

Fig. 13b

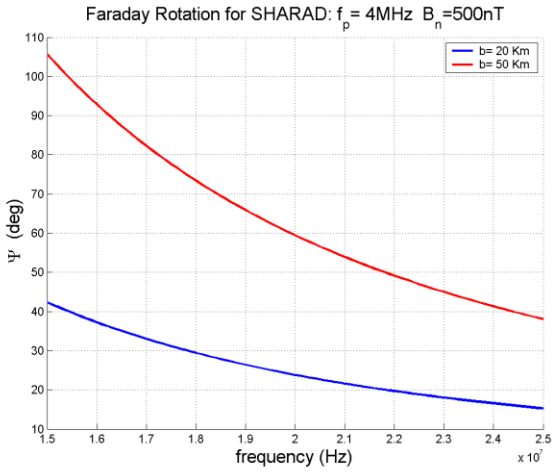

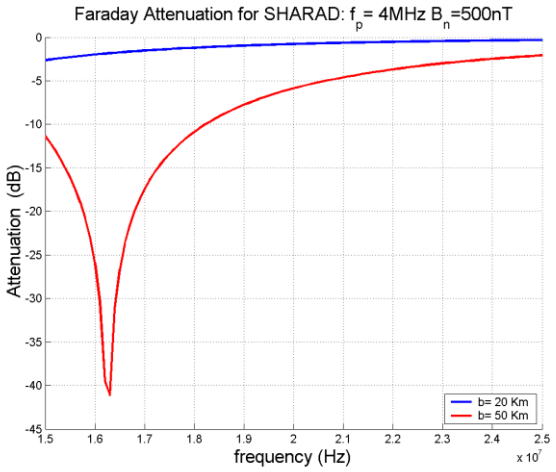

Fig. 13c

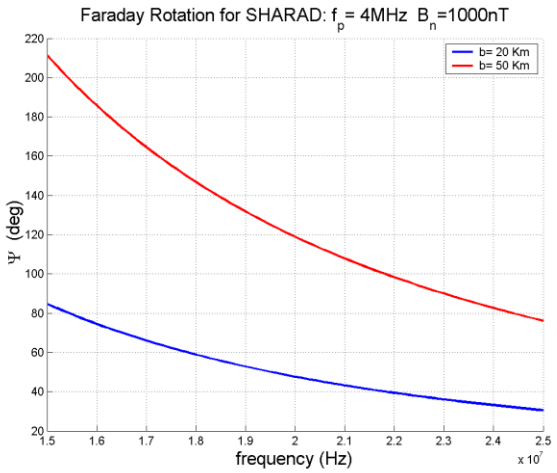

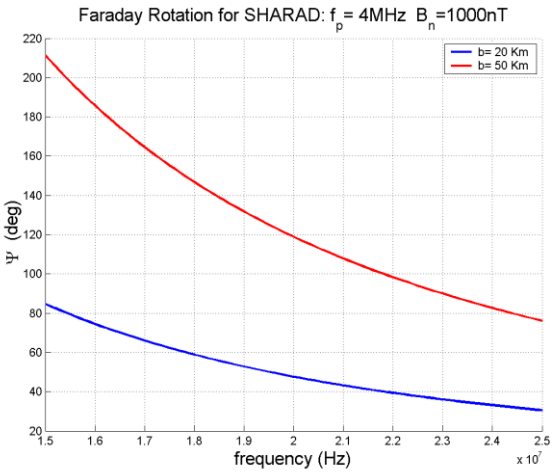

Fig. 13d

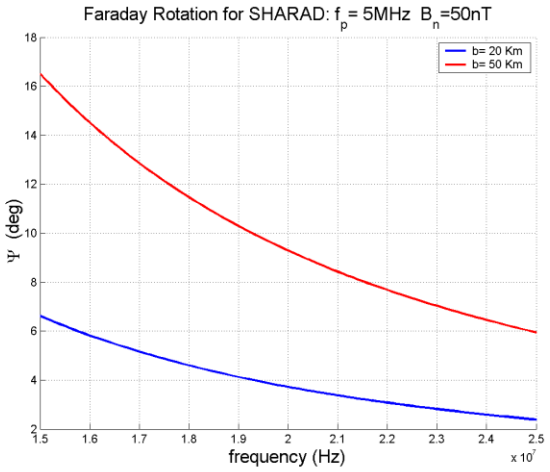

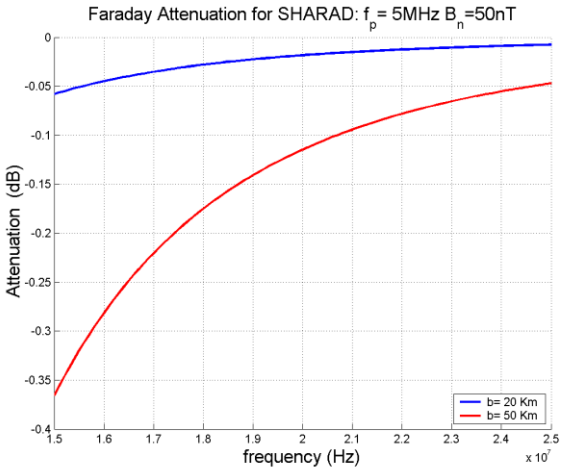

Fig. 14a

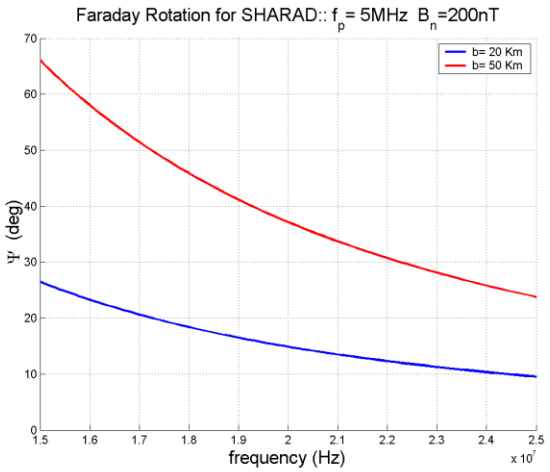

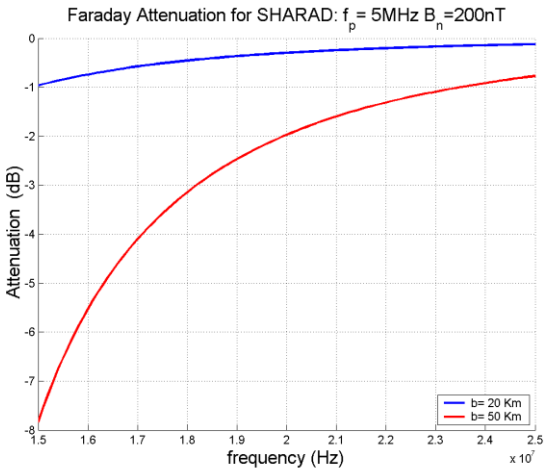

Fig. 14b

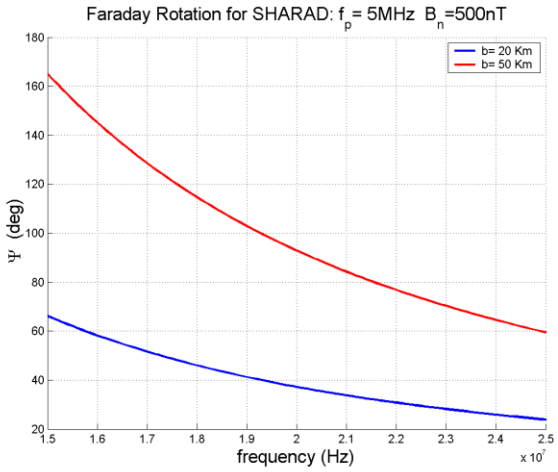

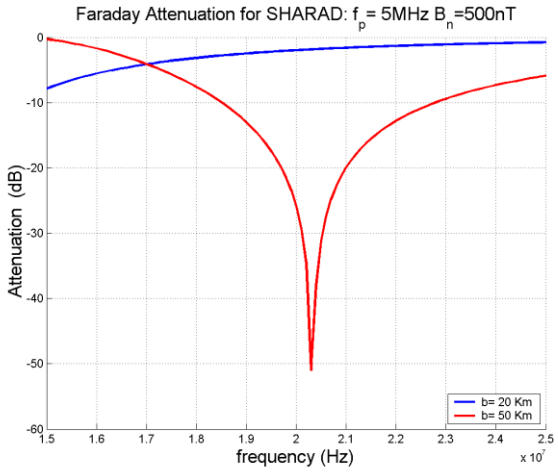

Fig. 14c

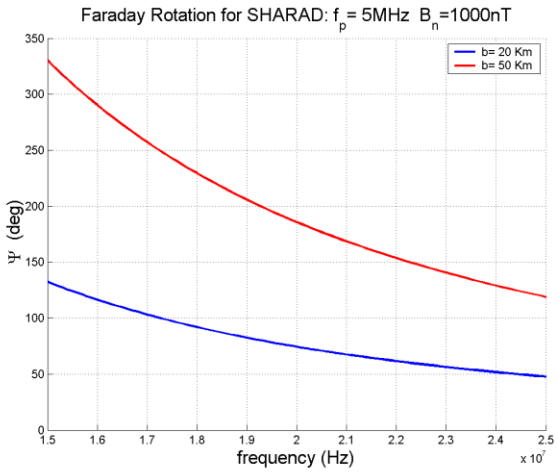

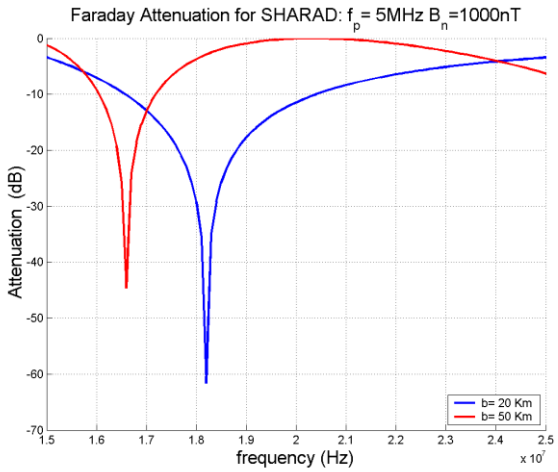

Fig. 14d